Applied Catalysis B: Environmental 121–122 (2012) 88–94

Contents lists available at SciVerse ScienceDirect

Applied Catalysis B: Environmental

journal homepage: www.elsevier.com/locate/apcatb

A non-acid-assisted and non-hydroxyl-radical-related catalytic ozonation with ceria supported copper oxide in efficient oxalate degradation in water

Tao Zhang [a], Weiwei Li [b], Jean-Philippe Croué [a,*]

[a] Water Desalination and Reuse Center (WDRC), King Abdullah University of Science and Technology (KAUST), Thuwal 4700, Saudi Arabia
[b] Research Center for Eco-Environmental Sciences (RCEES), Chinese Academy of Sciences (CAS), Beijing 100085, China

ARTICLE INFO

Article history:
Received 7 February 2012
Received in revised form 19 March 2012
Accepted 24 March 2012
Available online 2 April 2012

Keywords:
Catalytic ozonation
Acid assistance
Hydroxyl radical oxidation
Bicarbonate
Oxalate

ABSTRACT

Oxalate is usually used as a refractory model compound that cannot be effectively removed by ozone and hydroxyl radical oxidation in water. In this study, we found that ceria supported CuO significantly improved oxalate degradation in reaction with ozone. The optimum CuO loading amount was 12%. The molar ratio of oxalate removed/ozone consumption reached 0.84. The catalytic ozonation was most effective in a neutral pH range (6.7–7.9) and became ineffective when the water solution was acidic or alkaline. Moreover, bicarbonate, a ubiquitous hydroxyl radical scavenger in natural waters, significantly improved the catalytic degradation of oxalate. Therefore, the degradation relies on neither hydroxyl radical oxidation nor acid assistance, two pathways usually proposed for catalytic ozonation. These special characters of the catalyst make it suitable to be potentially used for practical degradation of refractory hydrophilic organic matter and compounds in water and wastewater. With in situ characterization, the new surface Cu(II) formed from ozone oxidation of the trace Cu(I) of the catalyst was found to be an active site in coordination with oxalate forming multi-dentate surface complex. It is proposed that the complex can be further oxidized by molecular ozone and then decomposes through intra-molecular electron transfer. The ceria support enhanced the activity of the surface Cu(I)/Cu(II) in this process.

1. Introduction

Catalytic ozonation with heterogeneous catalysts, a potential process to improve the degradation of recalcitrant organic pollutants in reaction with ozone in water, has attracted a lot of research interests in the last two decades [1]. This process is considered to follow either a hydroxyl radical oxidation pathway or a non-hydroxyl radical oxidation pathway. A number of mono- or composite metal oxides have been shown to be effective in accelerating ozone decomposition in water generating hydroxyl radicals [1–5]. Hydroxyl radical is useful in degrading a large number of organic compounds in water [6]. However, its reaction rates with saturated hydrophilic organic matter, e.g. ozonation products, are relatively low compared with its reaction with ozone ($k_{\bullet OH} = 1 \times 10^8$–$2 \times 10^9\ M^{-1}\ s^{-1}$) and bicarbonate/carbonate ($k_{\bullet OH} = 8.5 \times 10^6/3.9 \times 10^8\ M^{-1}\ s^{-1}$) [6], making the hydroxyl radical oxidation ineffective in the degradation of these organics. Catalytic ozonation not relying on hydroxyl radical oxidation is more suitable to effectively degrade the hydrophilic refractory organics, considering the ubiquitous hydroxyl radical scavengers in water.

With regard to catalytic ozonation not relying on hydroxyl radical oxidation, low molecular weight organic acids (e.g. oxalic, pyruvic, and succinic) are usually selected as model compounds, because hydroxyl radicals do not degrade these molecules effectively [7–11]. The reported catalytic ozonation with metal oxides like MnO_2 and Co_3O_4 are effective only at low pHs, i.e. below 3.5 [8–12]. Their activity declined significantly or was even totally inhibited when the pH was raised to neutral condition. This might be related to the surface properties of the catalysts and/or to the degradation pathway of the studied compounds. The pH_{pzc} of the catalysts are usually less than 7 (e.g. 5.6 for MnO_2 and 6.3 for Co_3O_4) [9,13]. The negatively charged catalyst surface at neutral pH hinders its interaction with the deprotonated model compounds. The degradation of the hydrophilic model compound is also subjected to acid-assistance, because H^+ is consumed in the decarboxylation reaction [7,10]. Catalysts that are efficient at neutral pHs and do not need the participation of H^+ in the catalytic ozonation have strong scientific interest and are of high practical value for the degradation of hydrophilic recalcitrant organics in water and wastewater.

CuO and supported CuO had been suggested in several references (experiments performed with 5,5-dimethyl-l-pyrroline-N-oxide (DMPO)) to be able to promote ozone decomposition generating hydroxyl radicals [14,15]. However, those experiments were conducted in pure water absence of buffer. Since the pH_{pzc} of CuO (normally being 9.5 [16]) was higher than the pH of the

* Corresponding author. Tel.: +966 02 808 2984.
E-mail address: jp.croue@kaust.edu.sa (J.-P. Croué).

0926-3373/$ – see front matter © 2012 Elsevier B.V. All rights reserved.
http://dx.doi.org/10.1016/j.apcatb.2012.03.021

reaction solutions, the pH of the solution was inevitably (although not indicated) raised by the CuO. OH^- is one of the critical species to induce ozone decomposition generating hydroxyl radicals in water [6]. Therefore, it is difficult to conclude from these references whether CuO itself can accelerate the hydroxyl radical generation from ozone. Ceria (CeO_2) is a good support for the three-way catalyst to treat automobile-exhausted gases [17]. Ceria itself has no catalytic activity in the degradation of saturated carboxylic compounds in water. Ceria supported PdO was found to be able to improve oxalate ($k_{O_3} = 0.04\,M^{-1}\,s^{-1}$, $k_{\bullet OH} = 7.7 \times 10^6\,M^{-1}\,s^{-1}$ [7]) degradation during ozonation, which was ascribed to the reaction between atomic oxygen formed on PdO and ceria-adsorbed oxalate [18]. This process is also subjected to acid assistance. It is still unknown whether other metal oxides (e.g. cheaper metal oxides) supported on ceria are also effective and can follow a similar or a different reaction pathway.

It was found in this study that ceria supported copper oxide was able to significantly improve oxalate degradation at neutral pH range during ozonation. Moreover, the reaction is not H^+-assisted and can be promoted by bicarbonate, which is quite different from catalytic ozonation with the reported metal oxides that follow non-hydroxyl radical oxidation. This finding suggests that more affordable metal oxides have practical application value for catalytic ozonation of hydrophilic recalcitrant organics in water. Based on our results obtained under various conditions and in situ characterization of the surface species during the reaction, a novel mechanism was proposed for the heterogeneous catalytic ozonation relying on neither acid assistance nor hydroxyl radical oxidation.

2. Experimental

2.1. Catalyst preparation

Ceria support was synthesized with a urea-hydrothermal method [18]. It had a BET surface area of 94 $m^2\,g^{-1}$, average particle size of 10 μm, and a pH_{pzc} (pH at which the surface is zero-charged) of 6.3. CuO/CeO_2 was prepared by impregnating the ceria particles with $Cu(NO_3)_2$ aqueous solution with incipient wetness. Different concentrations of the copper nitrate solution were used to prepare the CuO/CeO_2 of different CuO loadings. The impregnated oxide was dried at 120 °C and finally calcinated with air at 550 °C for 4 h. CuO particles were prepared by direct calcination of the dried $Cu(NO_3)_2$ at 550 °C for 4 h and then grinded. They are characterized by a BET surface area of 8.4 $m^2\,g^{-1}$, an average particle size around 6 μm, and a pH_{pzc} of 9.5.

2.2. Characterization

BET surface area of the metal oxides was determined on a Micromeritics ASAP2000 analyzer. pH_{pzc} was determined with acid-base titration. Average particle size was measured on a Mastersizer 2000 laser particle size analyzer. STEM (scanning transmission electron microscopy) pictures and EDX (Energy-dispersive X-ray spectroscopy) spectra taken on a Titan 80-300 transmission electronic microscope were used to characterize the dispersion of CuO on CeO_2. XPS studies for the characterization of copper valences were carried out with a Kratos Axis Ultra DLD spectrometer equipped with a monochromatic Al Kα X-ray source ($h\nu$ = 1486.6 eV) operating at 150 W, a multi-channel plate and a delay line detector under 1.0×10^{-9} Torr vacuum. Current–voltage scan of the metal oxides was performed on an electrochemical analyzer (600D, CH Instruments) with a three-electrode electrochemical cell (inductive glasses doped with the metal oxides as the working electrode, a platinum wire as the counter electrode, and a saturated calomel electrode as the reference) to characterize the oxidation potential of the metal oxides.

A PerkinElmer FTIR spectrometer (Spectrum 100) equipped with a Universal ATR accessory was used to characterize oxalate coordination with metal oxides in presence or absence of ozone in water. In situ Raman spectra of the metal oxides in presence or absence of ozone were taken on a confocal microscopic Raman spectrometer (Aramis, Horiba Jobin Yvon) with a 9 mW 633 nm laser light irradiation to study whether active oxygen species can be formed on the oxides. The ATR-FTIR and Raman analysis procedures for the samples followed that in Ref. [18].

2.3. Experimental procedure

Gaseous ozone was produced with an ozone generator (3S-A5, Tonglin Technology) from dried oxygen gas. Aqueous ozone solution was prepared in Milli-Q water at room temperature (21 °C) by continuously bubbling gaseous ozone into a glass cylinder. The aqueous ozone concentration was determined with an ultraviolet spectrometer (Hach 500) at 258 nm (molar absorbance coefficient = 3000 $M^{-1}\,cm^{-1}$). The desired steady ozone concentration in the Milli-Q water was controlled by adjusting the electric current of the ozone generator. Pre-determined volume of ozone stock solution and mass of catalyst were quickly mixed with tetraborate buffered oxalate solution in a glass reactor. The reactor was sealed and magnetically stirred during all the reaction time. Samples taken at each time-point were immediately filtered with 0.45 μm acetate-fiber syringe filters and then purged with pure N_2 to remove residual ozone. The filtration had no impact on the oxalate concentration. For ozone analysis in the samples, the filters were pretreated with 50 mL of the ozone stock solution to avoid any further ozone demand during the filtration. It was noticed that the filter had negligible impact on the aqueous ozone concentration after the pre-treatment.

2.4. Analysis

Ozone concentration in reaction solution was determined with the UV spectrometer at 258 nm after the 0.45 μm filter filtration, using the tetraborate buffer as zero background. Oxalate had no detectable absorbance at this wavelength and thus no impact on the ozone measurement. Oxalate was analyzed on a Dionex ICS-1600 IC equipped with an AS-15 column (2 mm i.d.). The mobile phase was 30 mM KOH at a flow rate of 0.35 mL min^{-1}. Atrazine, used as a probe compound of hydroxyl radical, was determined on a Waters HPLC equipped with a Symmetry C-18 column at a UV wavelength of 220 nm. The mobile phase was isocratic H_2O/acetonitrile at a volume ratio of 3/7 and a flow rate of 1.0 mL min^{-1}. Dissolved copper concentrations were determined on an ICP-MS (Agilent 7500). CuO contents of the catalysts were also determined with the ICP-MS after digestion with HCl + HNO_3 (v/v, 3:1), and HF in sequence.

3. Results and discussion

3.1. Effect of copper loading amount

Fig. 1A shows oxalate removal during catalytic ozonation with CuO/CeO_2 prepared with different CuO loadings. CeO_2 alone nearly had no activity in promoting oxalate degradation. The increase of CuO loading from mass percentage of 1–12% led to a significant increase of the oxalate removal rate, reaching 97% after 25 min of reaction under our experimental conditions. Further increase of the CuO loading reduced the oxalate removal efficiency by this catalytic ozonation process. These results show that an optimum CuO content exists for the catalyst. CuO alone can also improve oxalate removal, but to a much lower degree, which was similar to the

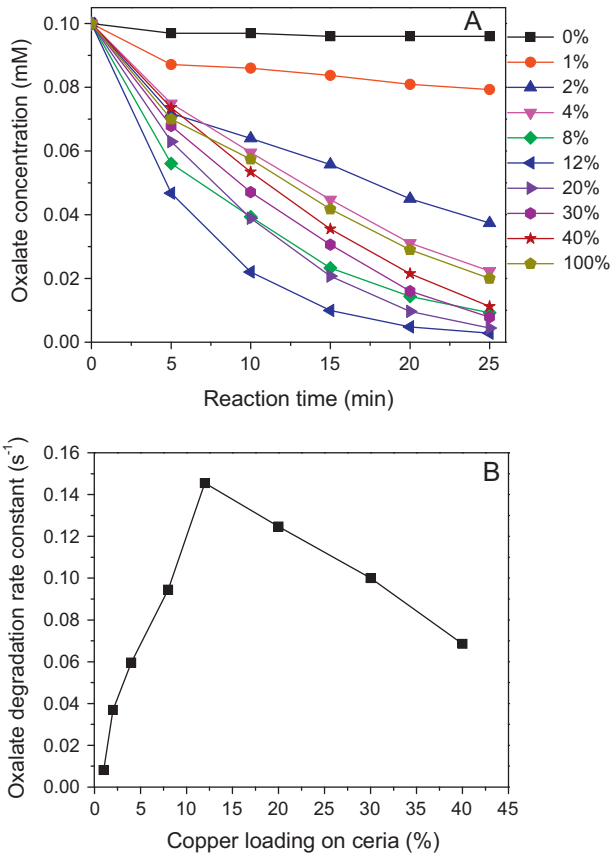

Fig. 1. Effect of CuO loading percentage of the catalyst on oxalate degradation (A) and the pseudo-first order degradation rate constant of oxalate (B) in catalytic ozonation. Experimental conditions: $[O_3]_o = 0.18$ mM, catalyst does = 200 mg L^{-1}, 10 mM tetraborate buffered pH 6.7, $T = 21$ °C.

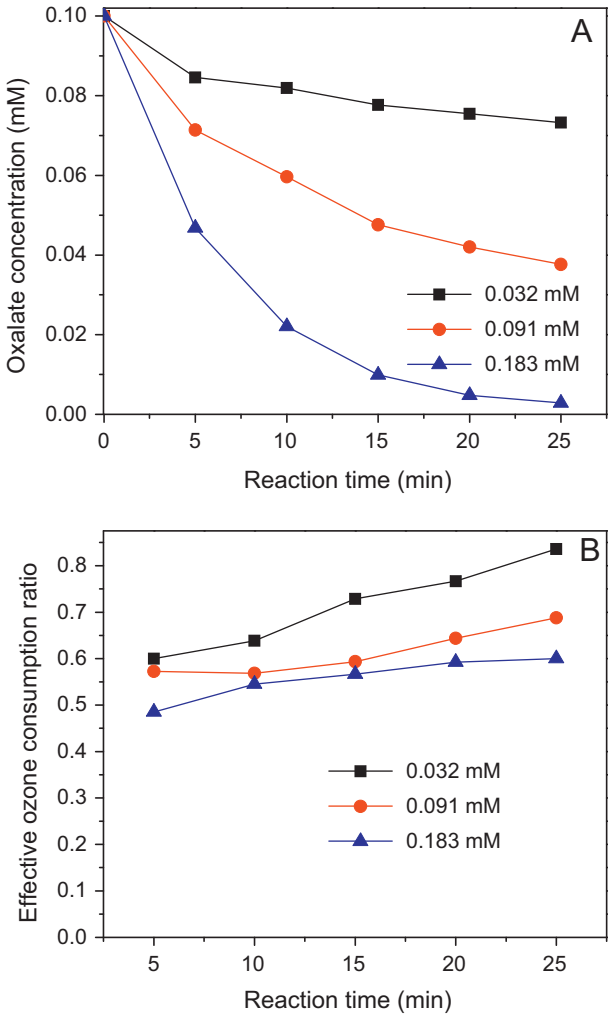

Fig. 2. Effect of ozone dose on oxalate degradation (A) and effective ozone consumption ratio (B) in $O_3/(CuO/CeO_2)$. Experimental conditions: catalyst does = 200 mg L^{-1}, 10 mM tetraborate buffered pH 6.7, $T = 21$ °C.

catalyst of 4% CuO content. Less than 2% oxalate was removed by adsorption alone onto these oxides (not shown here). The removal of oxalate observed during this catalytic ozonation process can be attributed to degradation but not adsorption phenomena. The ozone decomposition was also enhanced by the catalyst during the reaction (Supplementary material Fig. S1). However, unlike the oxalate degradation, the ozone decomposition rates seem to have no close relationship with the CuO loadings of the catalyst, suggesting that not all of the ozone consumption led to oxalate degradation in the catalytic ozonation. The oxalate degradation can be interpreted with pseudo-first order reaction model (with R^2 values > 0.97) for all CuO/CeO_2 with CuO loading over 1%. The corresponding reaction rate constants are shown in Fig. 1B. The reaction rate of the catalytic ozonation was raised by about 15 times, as the CuO loading of the catalyst was increased from 1% to 12%. The efficiency of the catalyst with 4% CuO content, which was comparable with CuO alone, was only 40% of the performance obtained with the optimized catalyst.

STEM pictures combined with EDX analysis revealed that the CuO was dispersed very well on the catalyst with CuO content no higher than 12% (Supplementary material Fig. S2). Further increase of CuO content led to obvious CuO agglomeration. The CuO agglomeration reduced its interaction with the CeO_2 surface, which was followed with the decline of the catalytic ozonation efficiency. Then, the interaction between the CuO and the CeO_2 surface seems to be critical for efficient catalytic ozonation. When used at the same dose, CuO/CeO_2 with 12% CuO content appeared to be 2.5 times more efficient than CuO alone indicating that the CeO_2 support improved the activity of CuO in the catalytic ozonation besides the surface dispersion effect. This optimized catalyst was used for following experiments without further specification.

3.2. Effect of ozone dose and catalyst dose

Fig. 2A and B shows oxalate degradation and the corresponding effective ozone consumption ratio (the molar ratio of oxalate degraded/aqueous ozone consumed) during catalytic ozonation at several ozone doses. The oxalate degradation rate increased significantly with the increase of ozone dose from 0.032 to 0.183 mM. The effective ozone consumption ratio decreased with the increase of ozone dose with the highest effective ozone consumption ratio being 0.84 in this ozone dose range. The negative effect of high ozone dose on the effective ozone consumption would be due to the limitation of the quantity of active sites for ozone activation or oxalate activation. Ozone can be consumed in reaction with OH^- (initiator of the ozone auto-decomposition reaction) and trace organic matter in the synthetic water, or even in reaction with ozone decomposition intermediates on the catalyst surface. These ozone consumptions are ineffective for oxalate degradation. If the active sites of the catalyst were limited for the catalytic ozonation of oxalate, more ozone would be consumed ineffectively in the water with the increase of ozone dose.

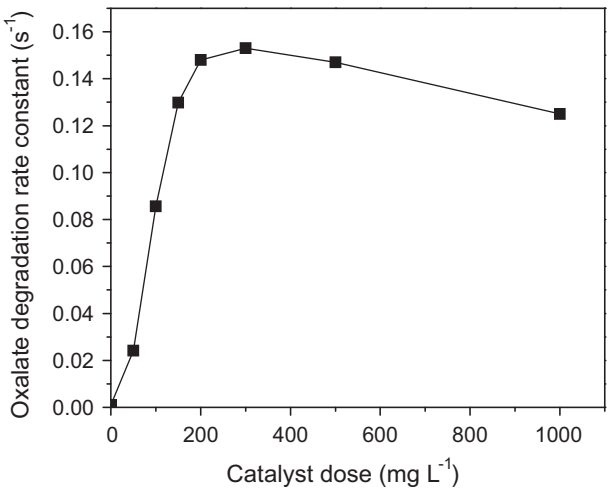

Fig. 3. Effect of catalyst dose on the pseudo-first order degradation rate constant of oxalate in O_3/(CuO/CeO_2). Experimental conditions: $[O_3]_o$ = 0.18 mM, $[oxalate]_o$ = 0.1 mM, 10 mM tetraborate buffered pH 6.7, T = 21 °C.

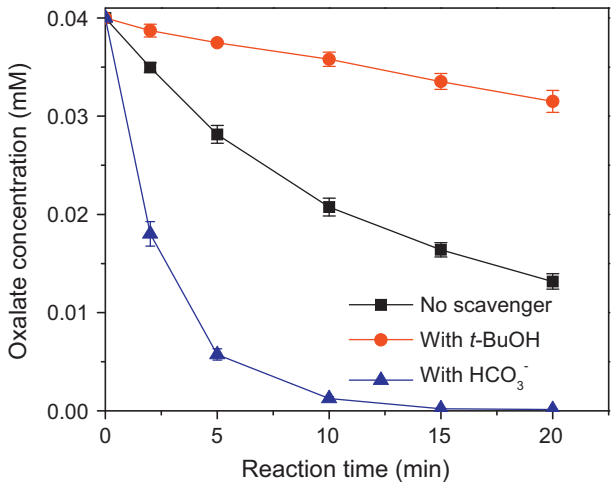

Fig. 5. Oxalate degradation in O_3/(CuO/CeO_2) in presence or absence of hydroxyl radical scavengers. Experimental conditions: $[O_3]_o$ = 0.09 mM, catalyst dose = 100 mg L^{-1}, $[t\text{-BuOH}]_o$ = 180 μM, $[HCO_3^-]_o$ = 5.0 mM, 10 mM tetraborate buffered pH 8.0, T = 21 °C.

There was a significant increase of the pseudo-first order degradation rate constant (from 0.024 to 1.48 s^{-1}) for the catalytic ozonation of oxalate, when the catalyst dose was increased from 50 to 200 mg L^{-1} (Fig. 3). As the catalyst dose was further increased to 300 mg L^{-1}, the rate constant increased only slightly, i.e. by 3%. The degradation rate constant slowly decreased as the catalyst dose was increased above 300 mg L^{-1}. The result suggests that increasing catalyst dose above certain amount would also lead to more ineffective ozone consumption for the oxalate degradation.

3.3. Effect of pH

Fig. 4 shows the oxalate removal for the catalytic reaction at different pHs. The catalyst showed the highest activity at pH 6.7 and 7.9. It declined significantly as the water solution became acidic or alkaline. There was only slight oxalate degradation at pH 9.2 and 3.2. After catalytic ozonation at pH 3.2, 5.3, 6.7, 7.9, and 9.2, the aqueous Cu^{2+} concentration were determined to be 1.47, 0.47, 0.19, 0.18 and <0.1 μg L^{-1}, respectively. More Cu^{2+} is leached from the catalyst at lower pHs. However, the activity of the catalyst declined significantly at low pHs. The result indicates that the trace

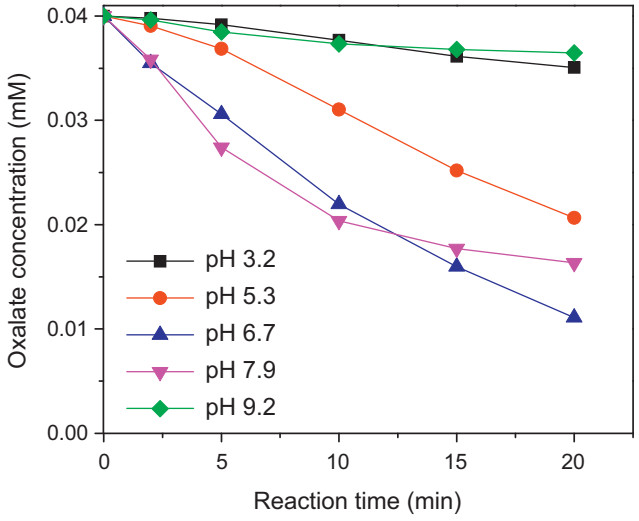

Fig. 4. Effect of pH on oxalate degradation in O_3/(CuO/CeO_2). Experimental conditions: $[O_3]_o$ = 0.07 mM, catalyst dose = 100 mg L^{-1}, 10 mM tetraborate buffered, T = 21 °C.

Cu^{2+} leached from CuO does not contribute in the overall catalytic ozonation.

Ozone decomposed very fast at pH 9.2 (Supplementary material Fig. S3), observation that can be largely attributed to the ozone reaction with OH^-, a major initiator for aqueous ozone decomposition into hydroxyl radical. Inconsistent with the rapid ozone decomposition, the oxalate degradation at this pH is quite limited. The result shows that hydroxyl radical is not effective in degrading oxalate. It cannot be the most critical oxidant species that induced significant oxalate degradation during the catalytic ozonation.

The pH_{pzc} of the catalyst was determined to be 9.1. The pKa_1 and pKa_2 of oxalic acid are 1.23 and 4.19, respectively. The activity decline of the catalyst with the decrease of pH seems to be related to the interaction of deprotonated oxalate with positively charged surface of the catalyst. Highly deprotonated oxalate will reasonably favor this interaction with the catalyst. Mono-deprotonated oxalate does not seem to be activated on the catalyst surface (i.e. Fig. 4).

Catalytic ozonation of carboxylates (including oxalate) with metal oxides had always been suggested to be most effective at low pHs [8–12,18]. The reaction efficiency usually declined significantly when the pH was raised to neutral pH. The carboxylates' degradation in catalytic ozonation was considered to be subjected to acid-catalysis, because H^+ participated in the degradation [7,10]. To the best of our knowledge, it is the first time that optimum catalytic ozonation for oxalate is reported to occur at neutral pH range with a new reaction pathway different from the acid-assisted one. The participation of H^+ seems to be unnecessary for the oxalate degradation in this catalytic ozonation with CuO/CeO_2.

3.4. Hydroxyl radical generation in the catalytic ozonation

Tert-butanol (t-BuOH) ($k_{\bullet OH} = 6 \times 10^8$ M^{-1} s^{-1}) and bicarbonate ($k_{\bullet OH} = 8.5 \times 10^6$ M^{-1} s^{-1}) are two hydroxyl radical scavengers that are usually used to differentiate molecular ozone oxidation from hydroxyl radical oxidation in ozonation [6]. The presence of t-BuOH significantly inhibited oxalate degradation in the catalytic ozonation (Fig. 5). In contrast, the presence of bicarbonate significantly improved the oxalate degradation.

The inhibition effect of t-BuOH on organic compound degradation is usually considered as a signature of hydroxyl radical oxidation in aqueous phase. However, as shown in Fig. 4, there was nearly no oxalate degradation occurring at pH 9.2, condition that favors the hydroxyl radical generation from ozone

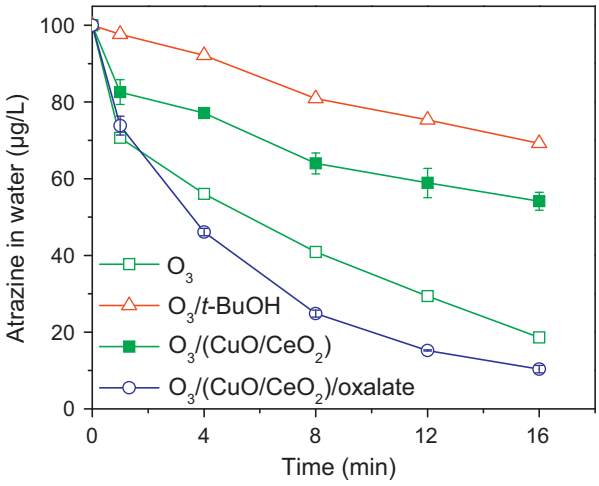

Fig. 6. Atrazine degradation in ozonation alone in presence or absence of t-BuOH and catalytic ozonation in presence or absence of oxalate. Experimental conditions: $[O_3]_o = 0.07$ mM, catalyst dose = 100 mg L^{-1}, $[t\text{-BuOH}]_o = 1.0$ mM, $[oxalate]_o = 0.01$ mM, 10 mM tetraborate buffered pH 6.7, $T = 21\,^{\circ}C$.

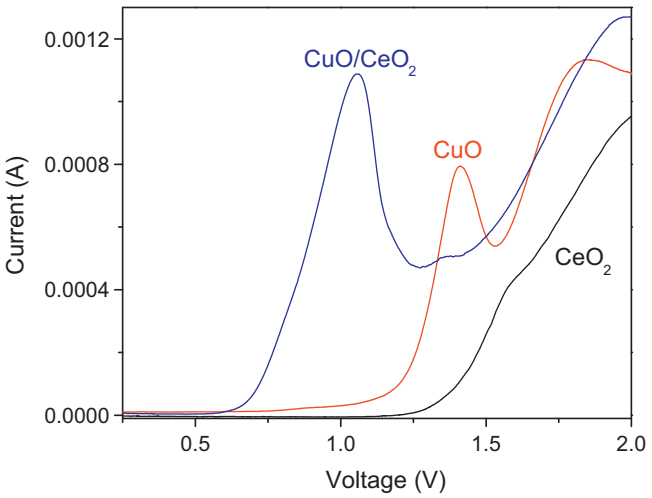

Fig. 7. Voltage–current relationship of CuO, CeO_2, and CuO/CeO_2 in 1.0 M $NaNO_3$ solutions saturated with N_2.

decomposition due to the ozone–OH^- reaction [6]. Therefore, the negative impact of t-BuOH cannot be attributed to its quenching effect on the hydroxyl radical generation in the catalytic ozonation process. A possible explanation to this finding could be the interference of t-BuOH on the interaction of ozone and oxalate with the catalyst surface.

The promotion effect of bicarbonate also indicates that the oxalate degradation in the catalytic ozonation cannot be ascribed to hydroxyl radical oxidation. Although bicarbonate can be oxidized by hydroxyl radical into bicarbonate radical, the latter radical species is not likely to be the main and direct oxidant responsible for the degradation of oxalate. This radical species has a lower reducing potential (1.78 V at pH 7.0 [19]) than ozone (2.08 V) and is only selective for electron-rich moieties, e.g. amine-, aryl-, and sulfur-containing compounds [6,20]. The promotion effect of bicarbonate is a new and interesting phenomenon for catalytic ozonation. It needs further detailed study to uncover the complete mechanism. At present, this promotion effect can be at least partly ascribed to the enhancement of the aqueous molecular ozone stability by bicarbonate (its inhibition on ozone self-decomposition is shown in Supplementary material Fig. S4), because bicarbonate can terminate the self-decomposition cycle of ozone by consuming hydroxyl radicals generated from ozone–OH^- reaction [6].

Atrazine ($k_{O_3} = 6\,M^{-1}\,s^{-1}$, $k_{\bullet OH} = 3 \times 10^9\,M^{-1}\,s^{-1}$ [6]) was used as a probe compound to further investigate hydroxyl radical generation in the $O_3/(CuO/CeO_2)$ reaction (shown in Fig. 6). Ozonation alone induced atrazine degradation in this experiment. Introduction of t-BuOH significantly reduced the atrazine degradation in ozonation alone, suggesting that most part of the atrazine degradation during ozonation was due to the hydroxyl radicals generated from ozone decomposition under this condition. The presence of the catalyst reduced the atrazine degradation rate compared with ozonation alone, indicating that the production of hydroxyl radicals from ozone decomposition was decreased by the catalyst. This result also supports the conclusion from Fig. 5. The atrazine degradation was improved when oxalate was present in the solution during catalytic ozonation, which means that hydroxyl radical is produced from the oxalate degradation. This phenomenon is consistent with the homogeneous catalytic ozonation of oxalate with Co^{2+}, where ozonide anion (O_3^-) was supposed to be the product of oxalate degradation and the precursor of hydroxyl radical [7].

Then, there would be two reasons accounting for the observed promotion of hydroxyl radical generation in catalytic ozonation with CuO in the Refs. [14,15]: (1) pH increase in the reaction solution because of the high pH_{pzc} of CuO and the absence of buffer, promoting ozone decomposition into hydroxyl radical; and (2) the degradation of trace oxalate (as one of the main ozonation products of the aromatic compounds [6]) produced hydroxyl radical as a by-product.

3.5. Discussion on the catalysis pathway

XPS data show the increase of Cu(I)/Cu(II) ratio when CuO was supported on CeO_2 (Supplementary material Fig. S5). The oxidation potential of the Cu(I) in the oxides was analyzed with current–voltage (CV) scan. Fig. 7 shows the CV curves of CuO, CeO_2, and CuO/CeO_2 in a N_2-saturated 1.0 M $NaNO_3$ solution. There was an oxidation peak for CuO alone at the voltage of 1.4 V, which can be ascribed to the oxidation of the trace Cu(I) to Cu(II) in the solid phase. When CuO is supported onto CeO_2, the oxidation peak shifted to 1.05 V. The result indicates that the valence electron of Cu(I) becomes more active, this status will then facilitate the oxidation of Cu(I) to Cu(II) by ozone compared with CuO alone.

Unlike the PdO/CeO_2 [18], we did not find any signal of atomic oxygen or peroxide on the surface of CuO and CuO/CeO_2 with in situ Raman spectra (Supplementary material Fig. S6). It is possible that O_3 abstracts one electron from surface Cu(I) to produce surface O_3^-. O_3^- usually reacts with H^+ to produce hydroxyl radical in water at pH less than 8 [6]. However, the hydroxyl radical generation was less in the catalytic ozonation mode than that in ozonation alone in absence of oxalate (shown in Fig. 6). We suspect that the surface O_3^- likely has less chance to react with H^+ because of the positive charge property of the catalyst in water at normal pHs, but might further react with another O_3 to produce reductive O_2^-. This kind of ozone decomposition will lead to more ineffective ozone consumption at high catalyst doses and a given ozone dose, thus reducing oxalate removal as shown in Fig. 3.

The newly formed surface Cu(II) from ozone oxidation is less saturatedly coordinated in the solid phase than the original surface Cu(II), because the original Cu(I) has a lower coordination number of lattice O^{2-} [21]. Consequently, it would be easier to form Cu(II)–oxalate complex at these sites. We observed a new band at 1640–1680 cm^{-1} for CuO/oxalate suspension in presence of ozone with ATR-FTIR, but not in absence of ozone (Fig. 8). Some references reported that Cu^{2+}-oxalate in a tetradentate bridging mode exhibited a strong vibration band between 1635 and 1670 cm^{-1} [22,23]. The new band appeared in presence of ozone located at

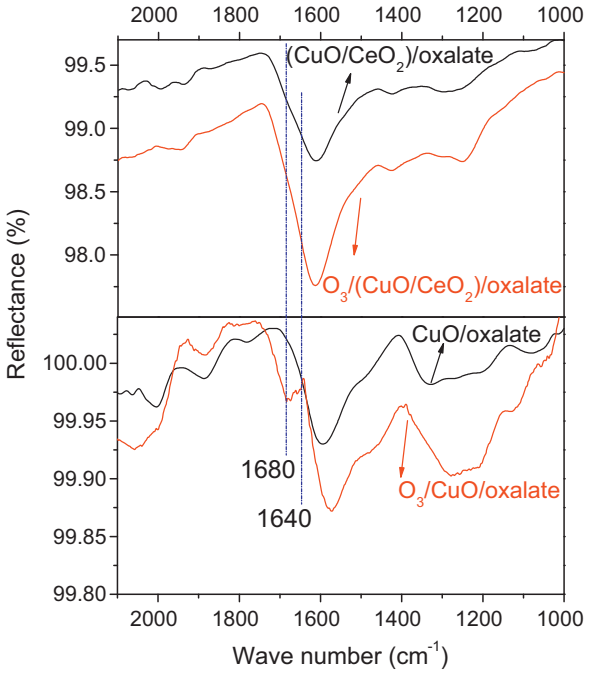

Fig. 8. ATR-FTIR spectra of CuO and CuO/CeO_2 in oxalate solution in presence or absence of ozone.

nearly the same position with the reported Cu^{2+}–oxalate complex. It would be reasonable to assign this new band to surface bridged Cu(II)–oxalate complex with unknown dentate number. Such a new band was not observed for the $O_3/(CuO/CeO_2)$, because it might have been covered by the strong peak of water adsorbed on the CuO/CeO_2 in that range (Fig. 8). Since effective oxalate degradation by catalytic ozonation occurred at pH above 5.3 (pKa_2 of oxalic acid being 4.19) (Fig. 4), the Cu(II)–oxalate complex in monodentate mode should be unreactive with ozone.

The ATR-FTIR spectra (around 1425 cm^{-1}) also show oxalate adsorption on the ceria support of the catalyst. We noticed oxalate adsorption on CeO_2 for catalytic ozonation with PdO/CeO_2 and ascribed oxalate degradation to the reaction of atomic oxygen (formed on PdO) with the adjacent CeO_2-adsorbed oxalate [18]. However, considering that there is no formation of active oxygen species on CuO (proved by the Raman spectra (Supplementary material Fig. S6)) and that CeO_2 itself has no activity in oxalate degradation [18], the oxalate adsorption on CeO_2 might be unimportant for the $O_3/(CuO/CeO_2)$. The results suggest that the newly formed Cu(II) should be active sites for the catalytic ozonation. Further experiments were conducted to compare the efficiency of the catalysts, with and without pre-ozone oxidation, on oxalate adsorption and on catalytic ozonation (Supplementary material Fig. S7). The amount of oxalate adsorbed onto the catalyst was increased by about 1.5 times after pre-ozonation. The oxalate removal rate also slightly increased by 20% after 20 min catalytic ozonation with the pre-ozonated catalyst compared with the non-pretreated one. This oxalate removal remained nearly the same when the catalyst was reused for 7 times in batch reactions (Supplementary material Fig. S8). Although the oxalate removal in adsorption alone increased after the pretreatment of the catalyst, it was still lower than 3% of the total removal achieved by catalytic ozonation. The slight improvement in oxalate degradation with the pretreated catalyst can thus be ascribed to the lower ozone demand required to oxidize the trace surface Cu(I) to the new Cu(II). The result suggests that the formation of the new Cu(II) on the catalyst through ozone oxidation can improve oxalate binding on the surface and promote its degradation by ozone. The decrease of the catalyst activity as CuO agglomerated (Fig. 1 and Supplementary material Fig. S2) can thus be ascribed to the reduction of the availability of surface Cu(I) in reaction with ozone producing active Cu(II) sites. The decrease of the oxalate degradation rate at catalyst doses over the optimum (Fig. 3) would be due to more ozone consumption in the oxidation of surface Cu(I) to the active new Cu(II) species.

Further Cu(II) oxidation in the catalyst to Cu(III) by molecular ozone may be considered impossible, because Cu(III) in the solid phase has a higher reducing potential (2.3 V) [24] than ozone. However, because the coordination of Cu(II) with an organic ligand usually reduces the redox potential of the Cu(III)/Cu(II) couple [25,26], this reaction may exist (Eq. (1)). Cu(III) complexes are highly unstable. The reaction involves one electron-transfer from the ligand to reduce the Cu(III) to the more stable Cu(II) [24,27]. Therefore, it is possible that the surface new Cu(II)–oxalate complex is oxidized by ozone to Cu(III)-oxalate which further dissociated into Cu(II) and oxalate radical through one intra-molecular electron transfer (Eq. (2)). The oxalate radical was reported to be very reductive having a high reaction rate even with molecular oxygen (Eq. (3)) [28]. The participation of H^+ is not necessary for this oxalate decomposition reaction. O_3^- would be formed in the ozone oxidation of Cu(II)–oxalate complex as a source of hydroxyl radical. This proposed mechanism consists with the phenomena shown in Figs. 4 and 6.

$$\equiv Cu(II)C_2O_4^{2-} + O_3 \rightarrow \equiv Cu(III)C_2O_4^{2-} + O_3^- \quad (1)$$

$$\equiv Cu(III)C_2O_4^{2-} \rightarrow \equiv Cu(II) + C_2O_4^{\bullet -} \quad (2)$$

$$C_2O_4^{\bullet -} + O_2 \rightarrow 2CO_2 + O_2^- \quad (3)$$

4. Conclusions

The results disclose a new catalytic ozonation pathway that relies on neither acid assistance nor hydroxyl radical oxidation for efficient degradation of the model hydrophilic refractory compound, oxalate, in water. Depending on this new pathway, CuO/CeO_2 exhibited special characters in the catalytic ozonation: (1) high efficiency at neutral pH, and (2) even higher efficiency in the presence of bicarbonate. These characters would make it suitable to be potentially used for normal waters to enhance the degradation of polar refractory organic pollutants and hydrophilic natural organic matter with high carboxylic contents (one of the precursors of disinfection byproducts that is difficult to be removed in conventional treatment processes [29]).

Acknowledgments

We want to thank Dr. Xu Zhao of Research Center for Eco-Environmental Sciences, Chinese Academy of Sciences, for his help in C-V determination. We also thank Mr. Qingxiao Wang, Dr. Mohamed N. Hedhili and Dr. Yang Yang of Imaging and Characterization Laboratory of KAUST for their help in performing STEM/EDX, XPS and Raman analysis, and Ms. Tong Zhan and Dr. Min Yoon of WDRC in ICP-MS and IC analysis.

Appendix A. Supplementary data

Supplementary data associated with this article can be found, in the online version, at doi:10.1016/j.apcatb.2012.03.021.

References

[1] J. Nawrocki, B. Kasprzyk-Horden, Appl. Catal. B 99 (2010) 27–42.
[2] T. Zhang, C. Li, J. Ma, H. Tian, Z. Qiang, Appl. Catal. B 82 (2008) 131–137.
[3] L. Yang, C. Hu, Y. Nie, J. Qu, Environ. Sci. Technol. 43 (2009) 2525–2529.
[4] L. Zhao, Z. Sun, J. Ma, Environ. Sci. Technol. 43 (2009) 4157–4163.
[5] M. Sui, J. Liu, L. Sheng, Appl. Catal. B 106 (2011) 195–203.

[6] U. von Gunten, Water Res. 37 (2003) 1443–1467.
[7] D.S. Pines, D.A. Reckhow, Environ. Sci. Technol. 36 (2002) 4046–4051.
[8] F.J. Beltran, F.J. Rivas, R. Montero-de-Espinosa, Ind. Eng. Chem. Res. 42 (2003) 3218–3224.
[9] R. Andreozzi, V. Caprio, A. Insola, R. Marotta, V. Tufano, Water Res. 32 (1998) 1492–1496.
[10] P.M. Alvarez, F.J. Beltran, J.P. Pocostales, F.J. Masa, Appl. Catal. B 72 (2007) 322–330.
[11] F. Delanoe, B. Acedo, N.K. VelLeitner, B. Legube, Appl. Catal. B 29 (2001) 315–325.
[12] F.J. Beltran, F.J. Rivas, R. Montero-de-Espinosa, Water Res. 39 (2005) 3553–3564.
[13] Y. Dong, G. Wang, P. Jiang, A. Zhang, L. Yue, X. Zhang, Bull. Korean Chem. Soc. 31 (2010) 2830–2834.
[14] J. Qu, H. Li, H. Liu, H. He, Catal. Today 90 (2004) 291–296.
[15] L. Zhao, Z. Sun, J. Ma, H. Liu, Environ. Sci. Technol. 43 (2009) 2047–2053.
[16] P.L. Brezonik, W.A. Arnold, Surface Chemistry and Sorption Process – Water Chemistry: An Introduction to the Chemistry of Natural and Engineered Aquatic Systems, Oxford University Press, New York, 2011.
[17] H.W. Jen, G.W. Graham, W. Chun, R.W. McCabe, J.P. Cuif, S.E. Deutsch, O. Touret, Catal. Today 50 (1999) 309–328.
[18] T. Zhang, W. Li, J.P. Croué, Environ. Sci. Technol. 45 (2011) 9339–9346.
[19] O. Augusto, M.G. Bonin, M. Amaso, E. Linares, C.C.X. Santos, S.L. De Menezes, Free Radic. Med. 32 (2002) 841–859.
[20] P. Neta, R.E. Huie, A.B. Ross, J. Phys. Chem. Ref. Data 17 (1988) 1027–1284.
[21] W.F. Schneider, K.C. Hass, J. Phys. Chem. 100 (1996) 6032–6046.
[22] K. Nonoyama, H. Ojima, K. Ohki, M. Nonoyama, Inorg. Chim. Acta 41 (1980) 155–159.
[23] M. Du, Y. Guo, X. Bu, Inorg. Chim. Acta 335 (2002) 136–140.
[24] T.V. Popova, N.V. Aksenova, Russ. J. Coord. Chem. 29 (2003) 743–765.
[25] A.E. Martell, Pure Appl. Chem. 17 (1968) 129–178.
[26] M. Orban, React. Kinet. Catal. Lett. 42 (1990) 343–353.
[27] D. Lowinsohn, M.V. Alipázaga, N. Coichev, M. Bertotti, Electrochim. Acta 49 (2004) 1761–1766.
[28] Y. Zuo, J. Hoigné, Environ. Sci. Technol. 26 (1992) 1014–1022.
[29] E.R.V. Dickenson, R.S. Summers, J.P. Croué, H. Gallard, Environ. Sci. Technol. 42 (2008) 3226–3233.